# Lecture 17
# Auger Electron Spectroscopy

Auger – history  cloud chamber

Although Auger emission is intense, it was not used until 1950's.

Evolution of vacuum technology and the application of Auger Spectroscopy - Advances in space technology

Various ways to estimate Auger electron kinetic energy

$$E_{KL1\,L23} = E_k^{(z)} - E_{L1}^{(z)} - E_{L23}\,(z + \Delta) - \phi_A$$
$$= E_k^{(z)} - E_{L1}^{(z)} - E_{L23}^{(z)} - \Delta[E_{L2,3}\,(z+1) - E_{L2,3}^{(z)}]$$

$$E_{xyz} = E_x - \tfrac{1}{2}\,(E_x(z) + E_y(z+1)) - \tfrac{1}{2}\,(E_2(z) + E_2(z+1)) - \phi_A$$

$\Delta$ has been found to vary from 0.5 + 1.5.

Relaxation more important than ESCA.

Auger energy is independent of sample work function. Electron loses energy equal to the work function of the sample during emission but gains or loses energy equal to the difference in the work function of the sample and the analyser. Thus the energy is dependent only on the work function of the analyser.

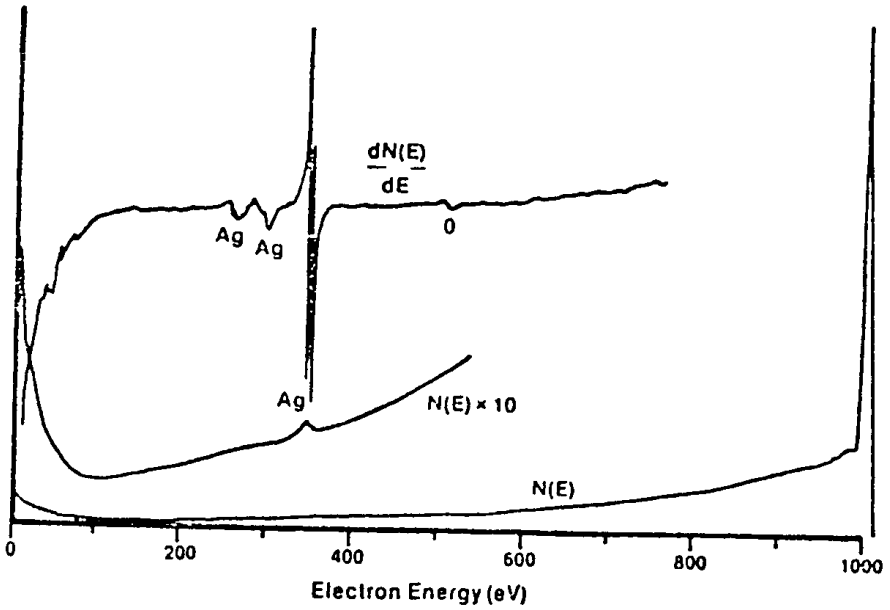


Fig. 1. Energy distribution and derivative of the energy distribution of secondary electrons from a silver target with an incident beam of 1000 eV electrons.

# Use of dN(E)/dE plot

# Instrumentation

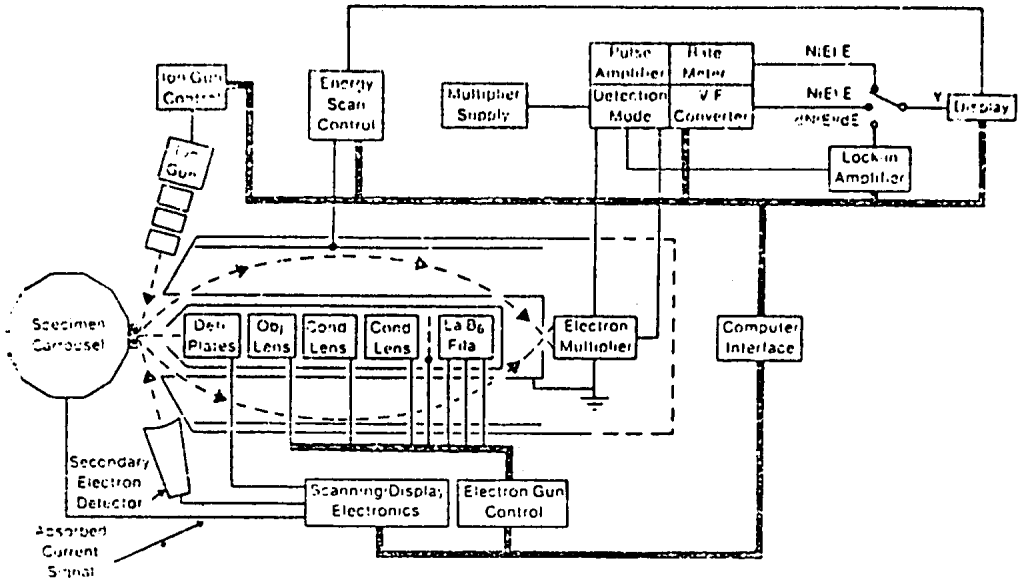


Fig. 4. Schematic layout of electron optics and electronics for a scanning Auger spectrometer.

# Early analysers

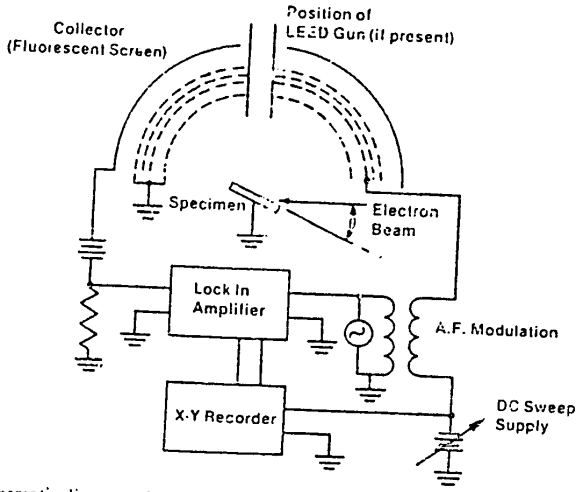


Fig. 5. Schematic diagram of a retarding field analyzer.

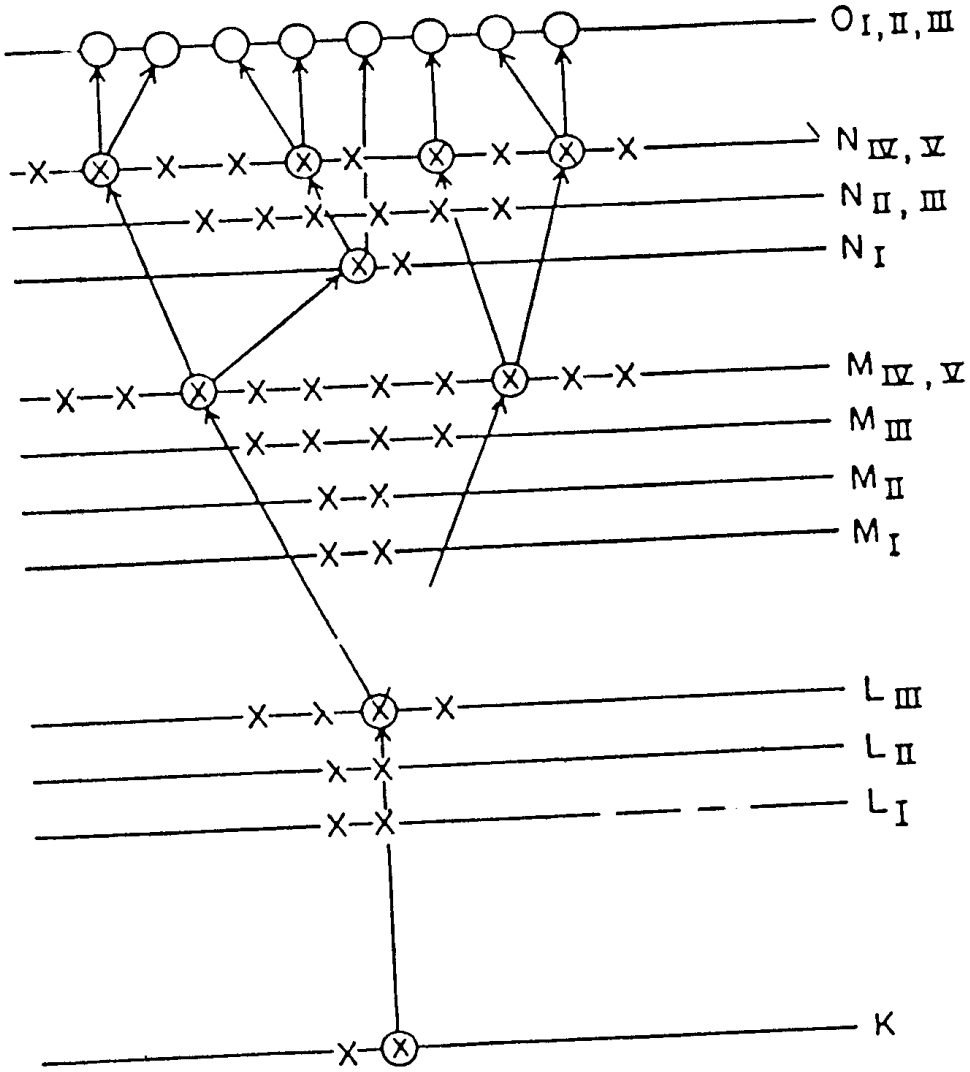


FIGURE 6.2. Schematic representation of a vacancy cascade in Xe. ×, Electrons; ○, vacancies; ⊗, vacancies that were subsequently filled by electrons.

What happens to the system after Auger emission

Chemical differences

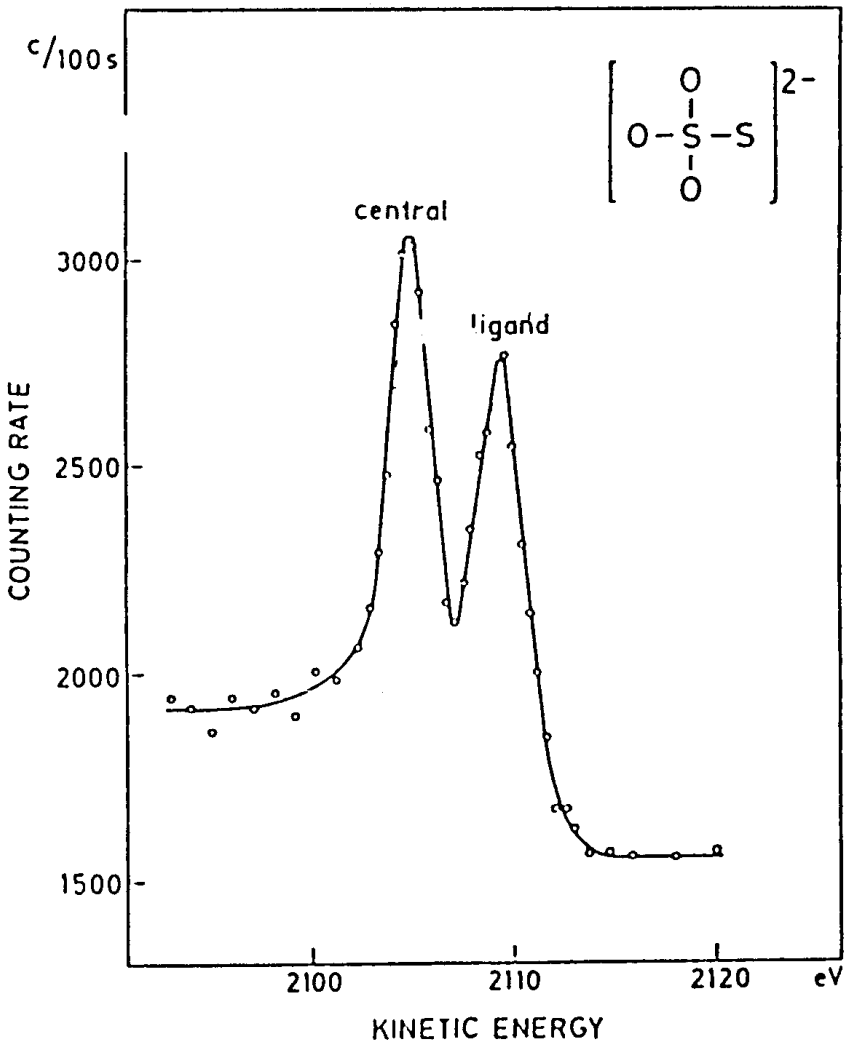


FIGURE 6.6. The *K–LL* [$2s^2 2p^4\ (^1D_2)$] Auger spectrum of sulfur for $Na_2S_2O_3$, showing two peaks corresponding to differences in chemical environment. [Reproduced from Fahlman *et al.*[32]]

When core electrons are involved in Auger, the chemical shifts are similar to XPS.

For $S_2O_3^-$, the chemical shifts between +6 and –2 oxidation states are 7eV for k shell and 6 eV for $\alpha_p$. The chemical shift for Auger is given as $\Delta E = \Delta E_1 - 2\Delta E\ (L_{II,III}) = 5$ eV

The experimental value is 4.7 eV

Chemical sifts of core levels - change in relaxation energy.

## Characteristics

Electron and photon excitation (XAES). Auger emission is possible for elements z >3. Lithium is a special case.
No Auger in the gas phase but shows in the solid state.

Auger emission from outer shells is constant with z. Thus KLL, LMM, MNN series etc can be used for elemental analysis.
Detection limits are 0.1 % atomic.

Spatial resolution ~ 50nm.

Depth resolution is better normal to the surface than in the plane.
Mean free path.

**Complications**

Plasmons, doubly ionized initial electron states, multiplet splitting, Multiple excitations, Coster-Kronig transitions. Super coster-Kronig transitions.

Volume and surface plasmons. Inter and intra band transitions or shake up

Coster – Kronig $L_1L_3$ X X $\neq$ L
Super Coster Kronig $L_1L_3$ X X = L
Cross over transitions. Eg. Mgo. Hole in O may be filled by electron from Mg - Non isotropic Auger emission from single crystals. Diffraction.
Isotropic from polycrystalline samples.

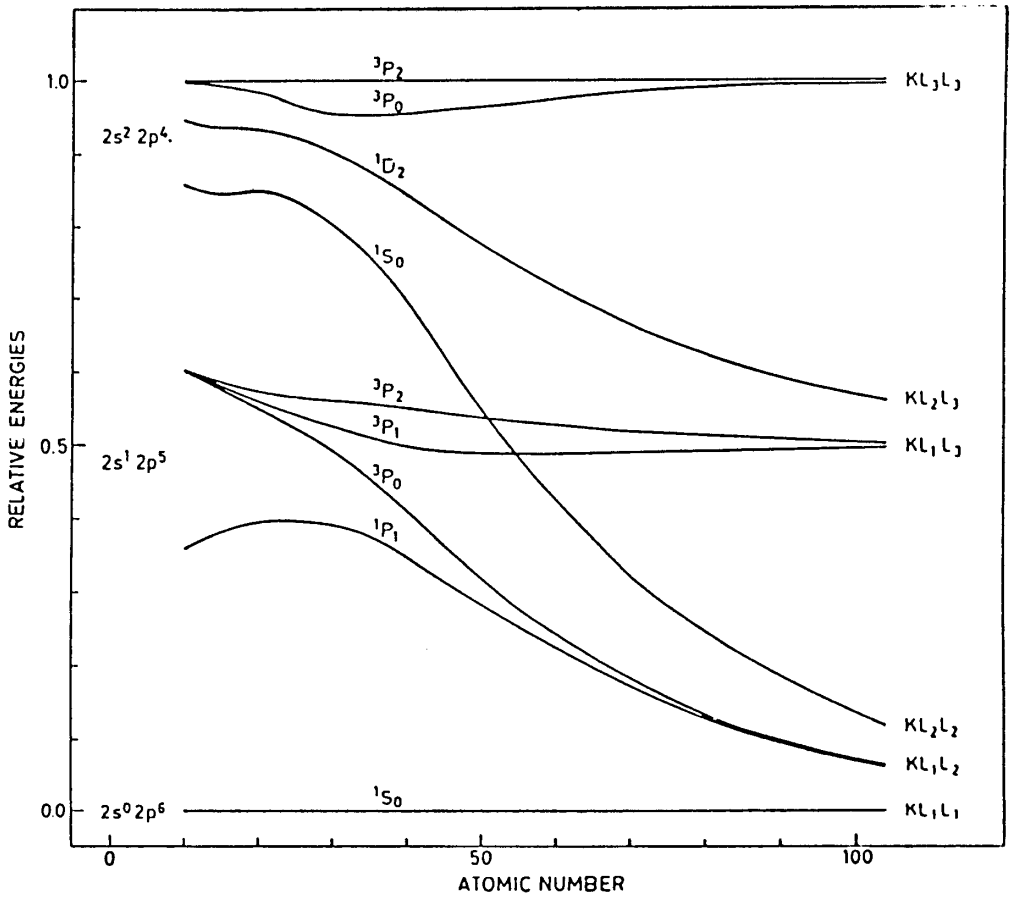


**FIGURE 6.1.** Relative line positions in *K–LL* Auger transitions as a function of *Z*. At low *Z* one has nearly pure *L–S* coupling and six lines. However, the $2s^22p^4\ ^3P$ is strongly forbidden in the nonrelativistic region. At high *Z* one has nearly pure *jj* coupling and six lines; nine lines are possible in the intermediate coupling region. [Reproduced from Siegbahn *et al.*,[13] Figure 4.1.]

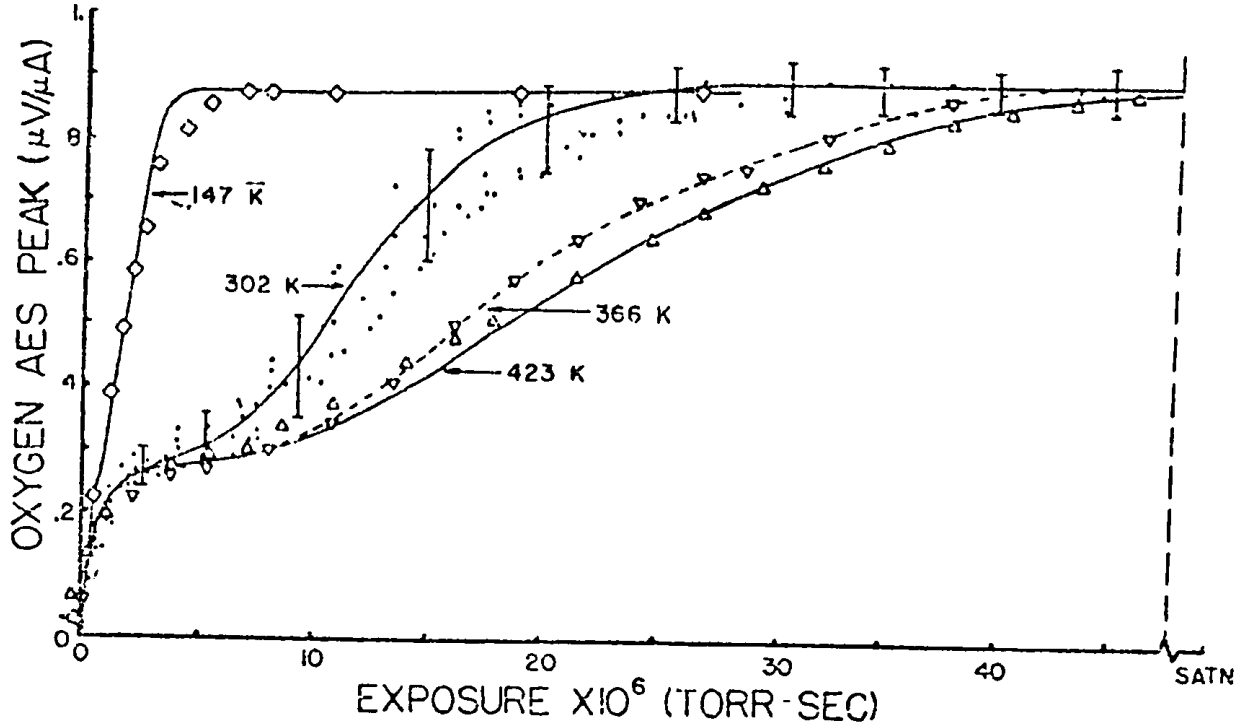


Fig. 8. Oxygen surface concentration versus oxygen exposure for Ni(100). (◇) 147 K, (⊙) 302 K, maximum and minimum limits for 302 K; (▽) 366 K; (Δ) 423 K. (From ref. 113)

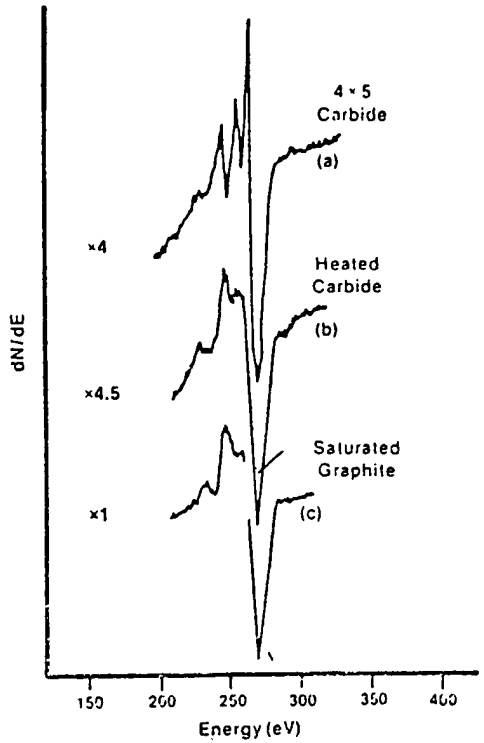


Fig. 34. Carbon KVV Auger spectra of the carbide and graphite forms of surface carbon on Ni(110). (a) Auger spectrum of a (4 × 5) C-saturated carbide surface formed at 550 K by a doser exposure of $C_2H_4$ equivalent to 200 L. (b) Graphite Auger spectrum formed by heating a saturated carbide layer to 775 K for 15 s. (c) Auger spectrum of a saturated graphite surface formed at 725 K by a doser exposure of $C_2H_4$ equivalent to 180 L. The energy of the incident electron beam was 2·0 keV and the modulation voltage was 2·0 V r.m.s., except (b) which had 3·0 V r.m.s. The indication of the relative signal magnitude has been corrected for the difference in modulation [illegible] that the $dN/dE$ signal was proportional to the square of the modulation

## Chemical effects

Relaxation is larger than in XPS. Chemical effects in XPS will not directly correspond with those of Auger. The difference between XPS and Auger energies is called Auger parameter, used to characterise the chemical state. More changes for transitions involving valence states.

Applications in:

Corrosion
Adhesion
Catalysis
Chemical characterization
Surface reaction
Electronic materials

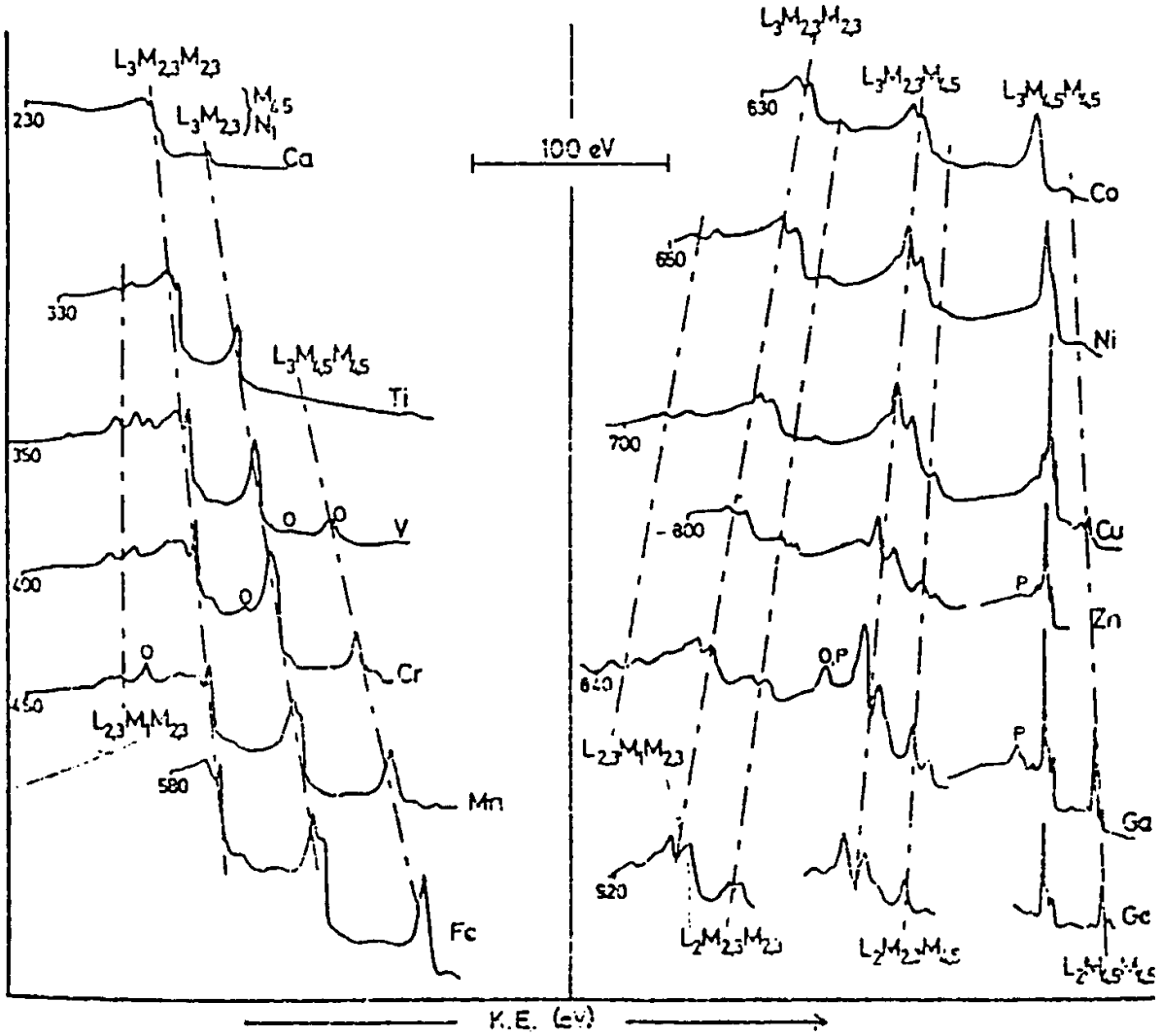


Fig. 18. LMM Auger spectra of elements Ca to Ge. Spectra of samples with low contamination levels have been chosen but some of the peak labelled O may contain contributions from oxygen XPS and Auger peaks. Peaks labelled P are due to plasmon-like energy losses. All spectra, except that of Ge, were recorded with instruments retarding the electrons to a constant analyser pass energy (increased sensitivity at low K.E.) Sources of spectra: Ca, Ti, Cr, Mn, Co, Cu (ref. 82); V (refs 82, 189, 218); Fe (ref. 189); Ni (refs 82, 218); Zn (refs 53, 123, 219, 220); Ga, Ge (refs 82, 53)

High resolution AES using photons

Beam effects
Electron stimulated desorption
Core hole lifetimes are smaller than vibrational time scale and dissociation is not important. But the core hole will lead to electron cascade and multiply charged ion many result which will have a large dissociation probability.

Photon induced desorption is also important but photon fluxes are much lower. Beam effect are important.

Excitation cross sections in XAES and EAES are different.

## Valence band information

In Auger of the type KLV, only one hole is created in the valence band. The Auger spectrum reflects the density in the valence band in spectra such as $L_{2,3}M_{4,5}M_{4,5}$ for transition metals such as Sc to Cu, the interaction between the two holes is important. e-e interactions determine the properties of such solids. The metal can be treated as a collection of atoms with individual configurations and a number of electrons fluctuating rapidly as a result of their interaction. The interaction can be described as coulomb interaction Ueff which is defined as Ueff = $\varepsilon^+ + \varepsilon^-$

$\varepsilon^+$ is the energy required for the transfer of an electron from fixed level (eg. $E_F$) to an atom in the average configuration and $\varepsilon^-$ is for the reverse transfer.

With W as the band width, if Ueff << W, the material is like a free electron metal with delocalised electrons and weak correlation. If Ueff >> W, the material behaves like localised electron material.
If we regard Ueff as energy difference between two states, one with two holes and other with two electrons on the atoms, then Ueff is related to the energy of the Auger process.

Core level line shapes

Core level AES for gases and solids are similar. Lifetime broadening is similar, relaxation and energy loses result in distinct effects.

Life time broadening, Lorentzian

$I(E) = I(E_0).\Gamma_L^2 / [(E-E_0)^2 + \Gamma^2]$

I(E) – intensity at E

$E_0$ – peak centre

$\Gamma_L$ – core hole life time broadening and one half of FWHM

½ FWHM = $\Gamma_L = h/\tau = (6.58 \times 10^{-16}) / \tau$ eV

$\tau$ – lifetime involved, in seconds.

Phonon broadening, Gaussian

$$I(E) = I(E_0) \exp [-(E-E_0)^2 / 2\Gamma_{ph}^2]$$

Extrinsic and intrinsic (shake up)

Plasmons

Added to instrument function.

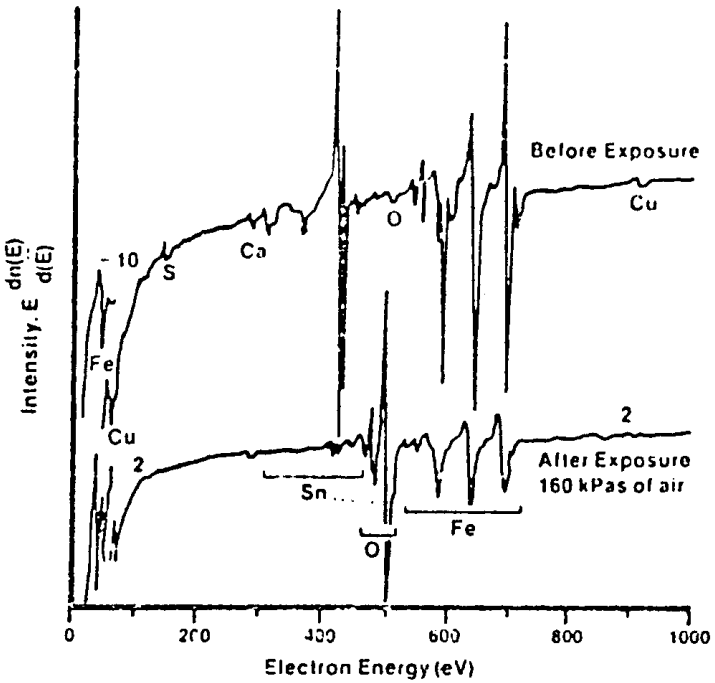


Fig. 6. Auger electron spectra from iron with two monolayers of adsorbed tin before and after exposure to 160 kPa of air. (From ref. [64])

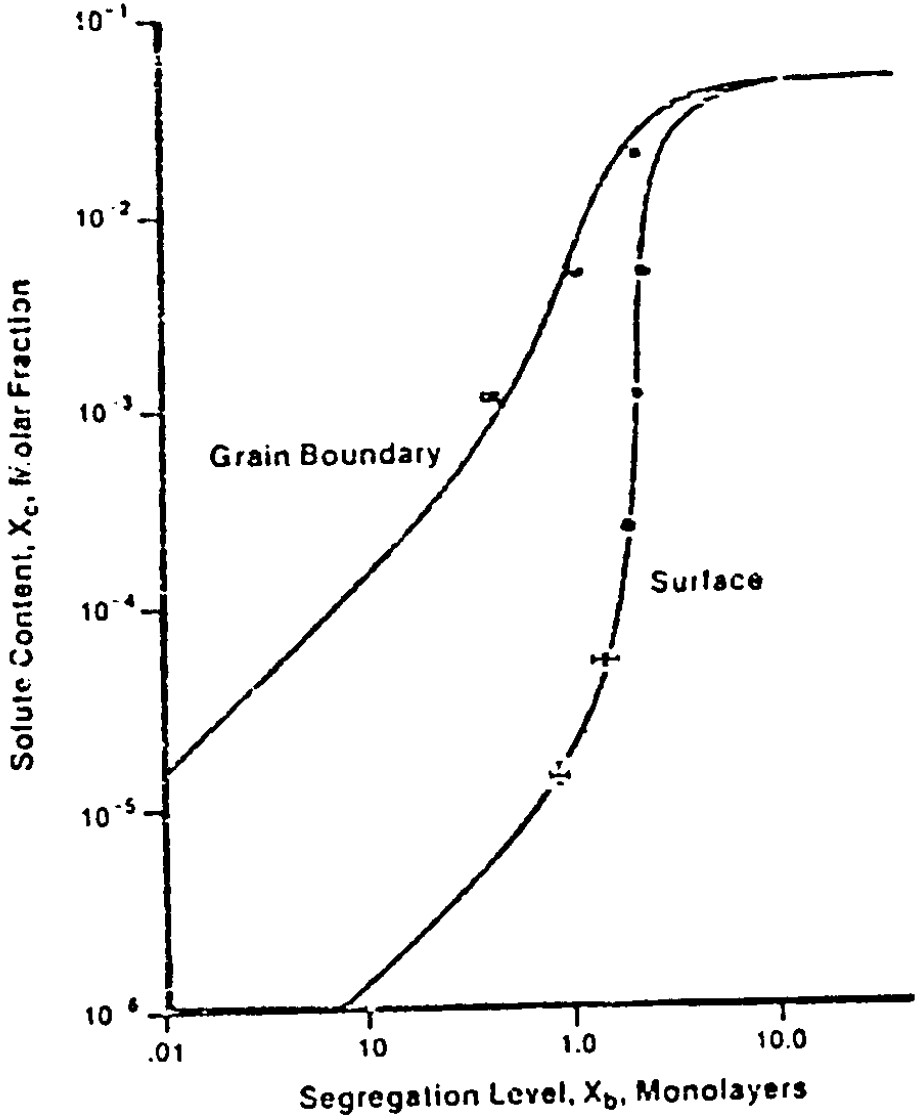


Fig. 7. The measured and theoretical equilibrium surface and grain boundary segregation levels as a function of tin solute content in iron, at 550 C. (From ref. 107)

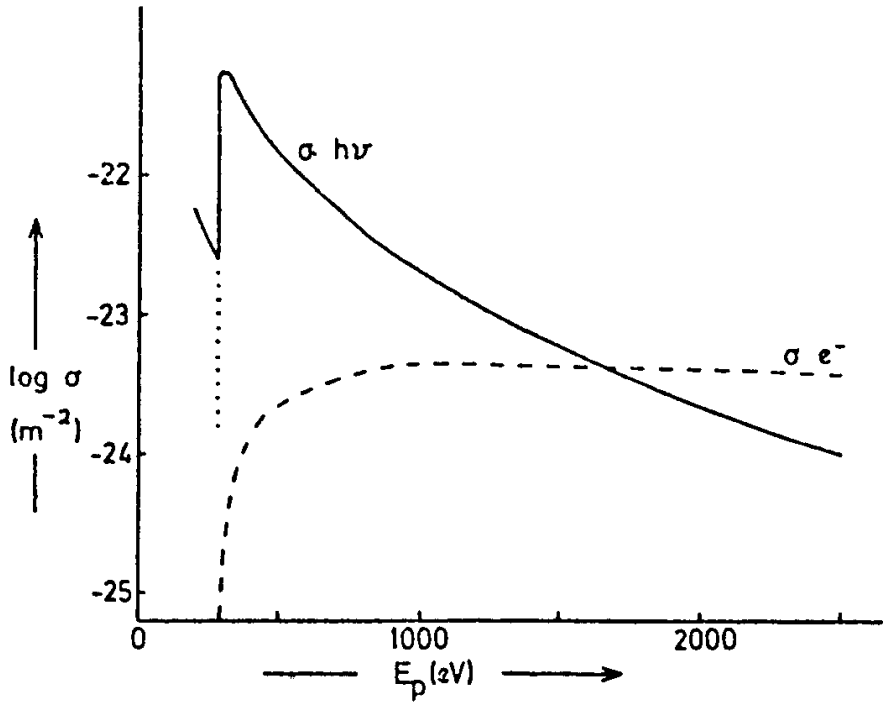


Fig. 3. Ionization cross-sections for the C 1s level. The Gryzinski formula[31] has been used to calculate the curve (dashed) for electrons. For photons absorption measurements[35, 36] have been used and all absorbing processes contribute to the observed cross-section. However, valence electron processes are only important below 280 eV where the C 1s ionization cross-section drops to zero, as shown by the dotted curve.

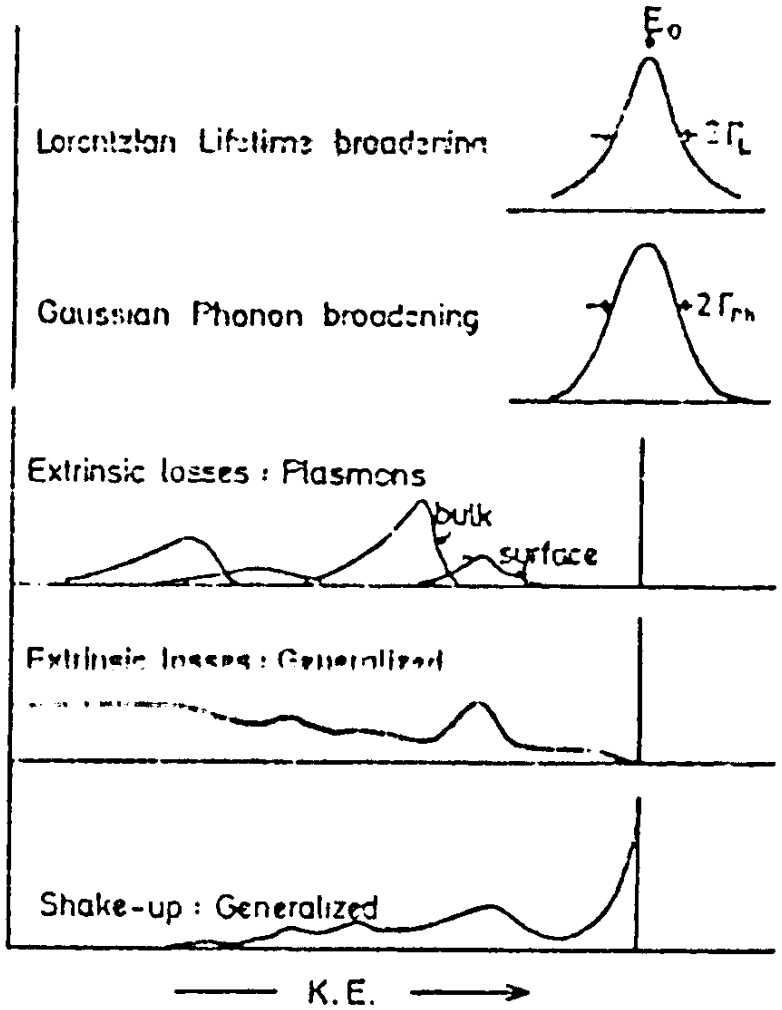


ig. 10. Summary of the effects on line shapes in electron spectroscopies. Note that phonon adening is associated with an energy shift not shown here.

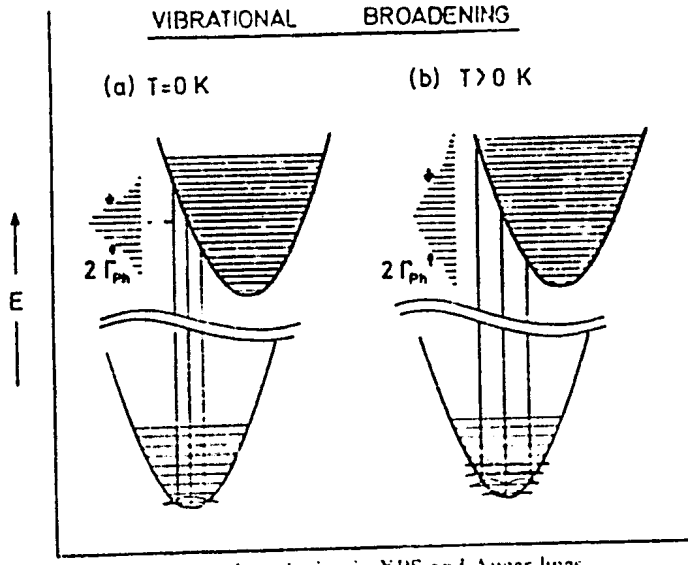


Fig. 11. The origin of phonon broadening in XPS and Auger lines.

## Threshold effects in Auger

Decay of the core hole leading to double ionization post collision effects changing peak energies.

$L_{2,3}$ spectra of Mg with Mg $K_\alpha$ and Al $K_\alpha$.

Double ionization satellite in Al $K_\alpha$ not in Mg $K_\alpha$.

By electrons it is found that the threshold for double ionization is ~120 eV, but the satellite was not sharp as with X-ray excitation.

When KE of outgoing electron is low, Auger emission can happen in the field of receding electron. Energy available can be re-partitioned. If threshold electron is used, Auger emission happens in the field of The receding electron. These interaction are called post collision interactions.

## Plasmon gains and losses

Plasmon gain occurs by intrinsic mechanism. For it to occur, plasmon excited should be at the site of ionization, therefore it cannot be extrinsic.

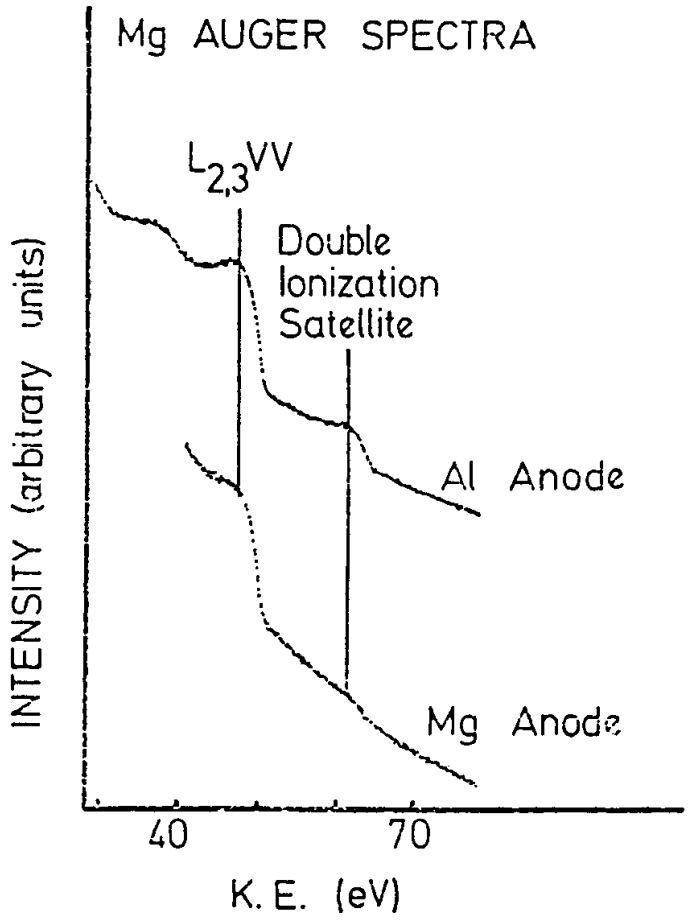


Fig. 13. Increase of the Mg LVV double ionization satellite intensity in XAES as the exciting X ray energy is increased above the Mg K ionization threshold.[175]

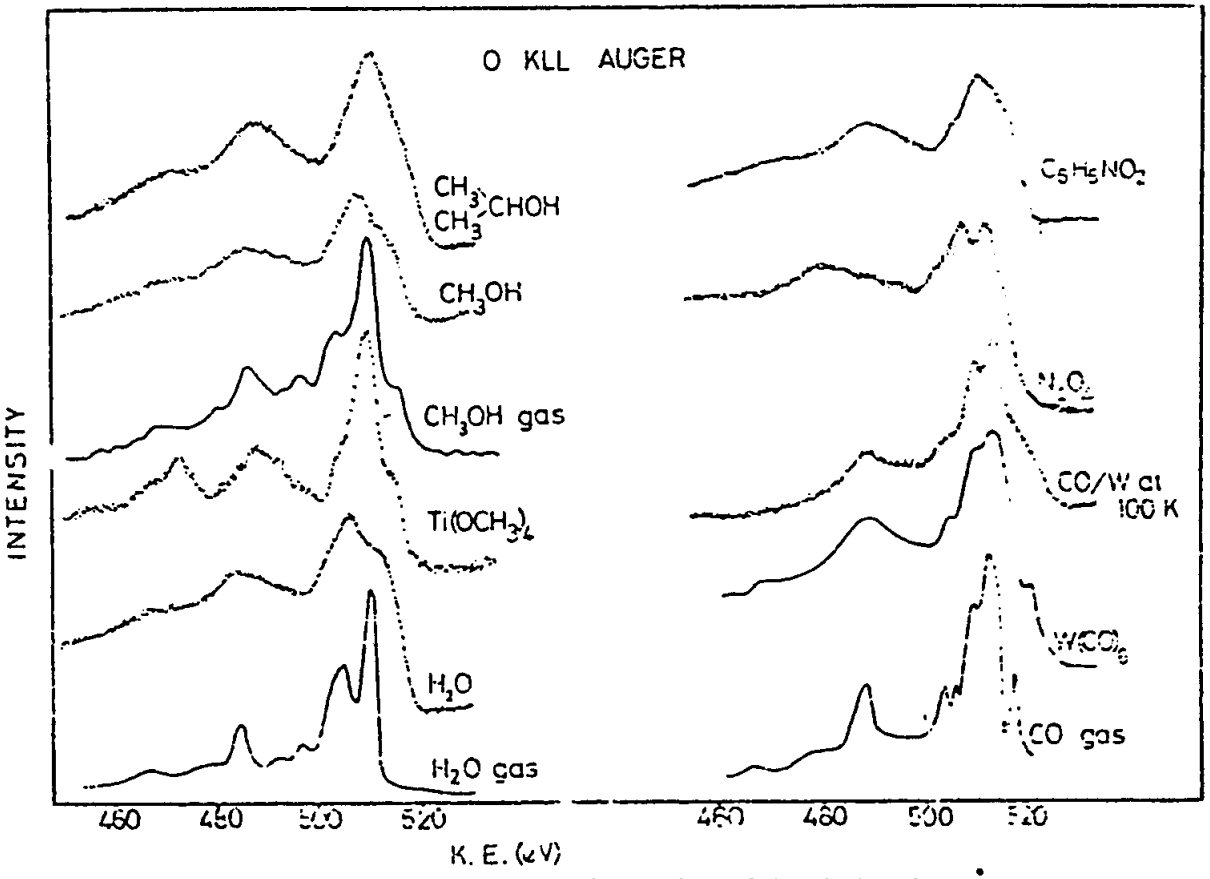


Fig. 26. O KLL Auger spectra from oxygen in a variety of chemical environments. All [illegible] are from condensed layers unless otherwise stated. The spectra of $H_2O$ gas, $CH_3OH$ [illegible] and CO gas have been shifted by respectively approximately 12, 11, and 16 eV to higher K.E. to allow for the different reference levels and relaxation effects (Section III.F) and to line up the characteristic features as well as possible. Differences in the low K.E. background are not significant as different instruments have been used to record the spectra. References: $H_2O$ gas (79, 253, 254); $H_2O$, $Ti(OCH_3)_4$, $CH_3OH$, $(CH_3)_2CHOH$, $W(CO)_6$, $N_2O_2$, and $C_5H_5NO_2$ (234); $CH_3OH$ gas (241, 242); CO gas (241, 255)

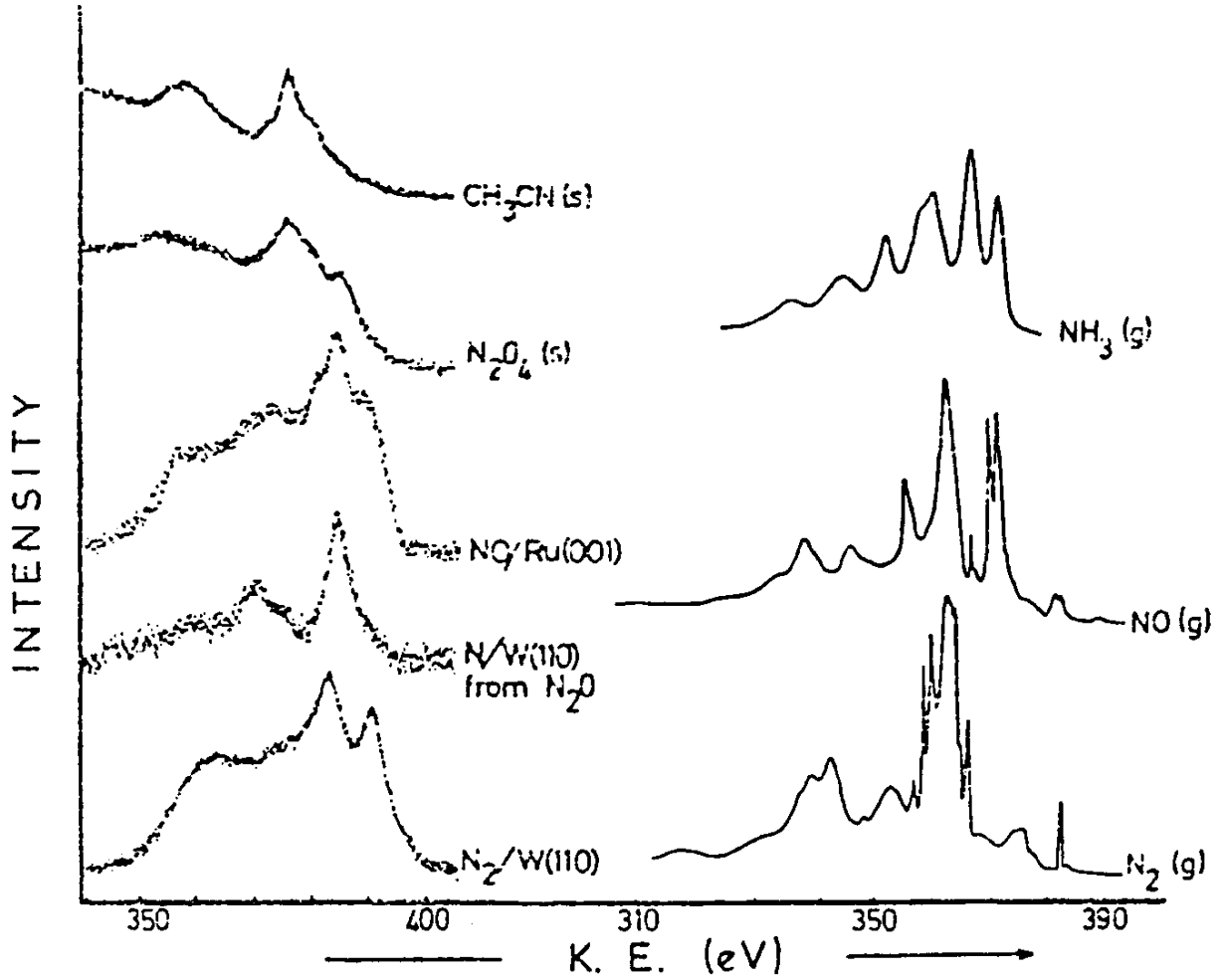


Fig. 27. N KLL Auger spectra from nitrogen in a variety of chemical environments. References $NH_3$ gas (259); NO and $N_2$ gas (258); $CH_3CN$ and $N_2O_4$ (234); NO Ru(001) (252); N/W(110) (249) $N_2$/W(110) (249, 260).

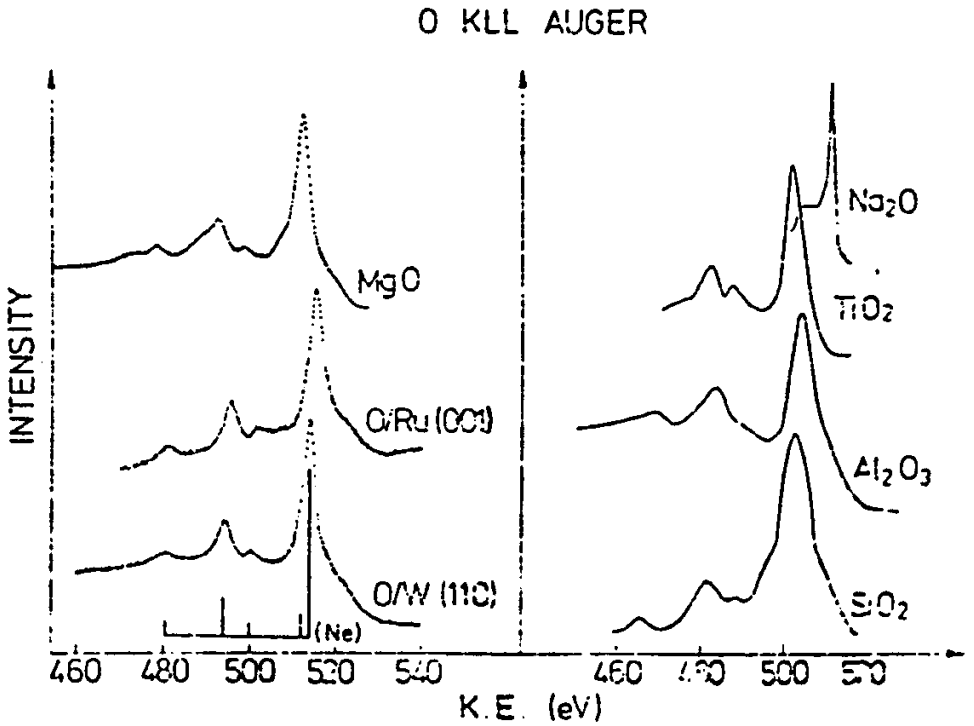


Fig. 23. Oxygen KLL Auger spectra from MgO,[231,232] oxygen chemisorbed on Ru(001)[236,245] and W(110),[248] $Na_2O$,[84] $TiO_2$,[97] $Al_2O_3$,[82] and $SiO_2$.[235] The *relative* spacings and intensities of Ne KLL lines[170] are also shown.

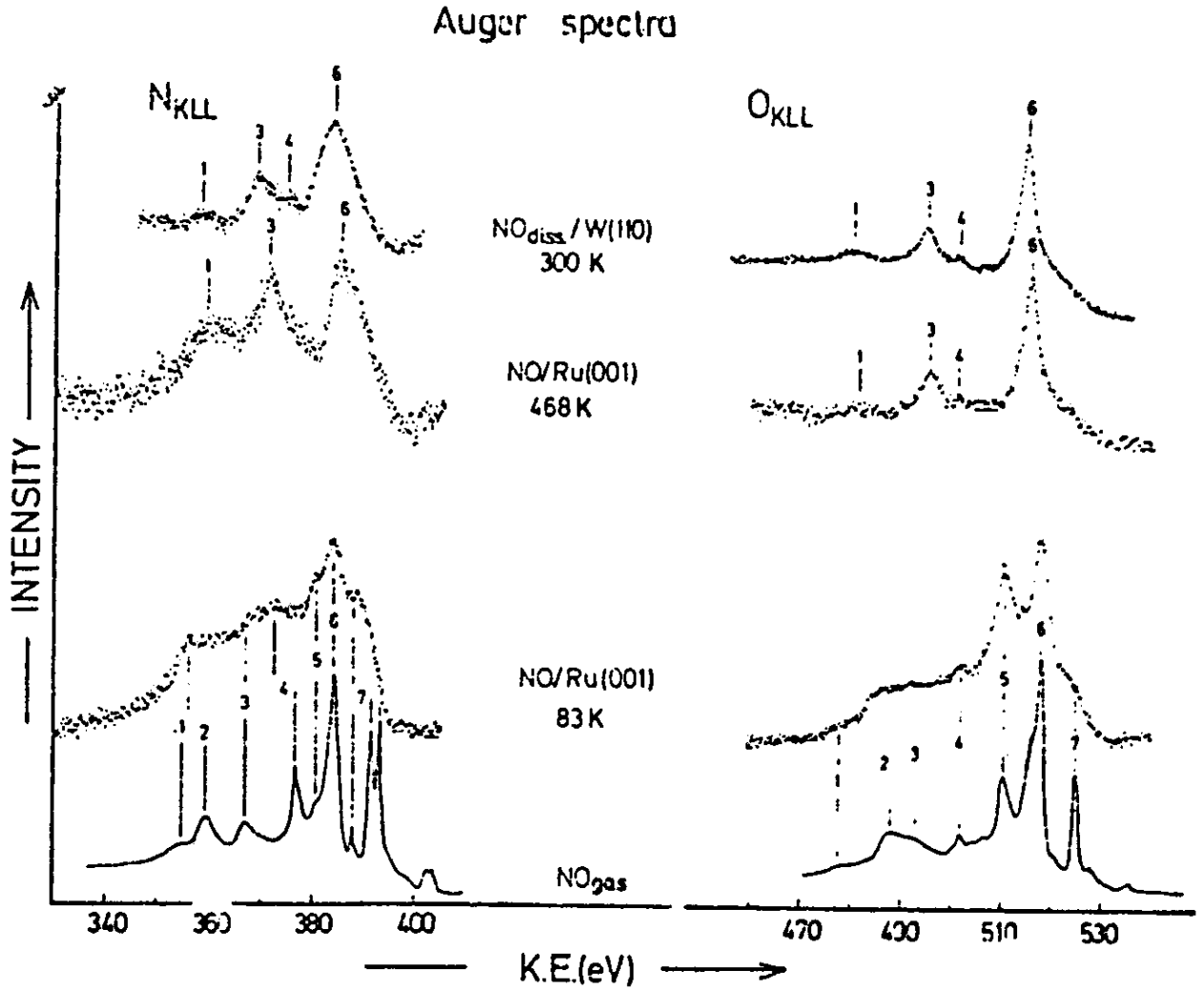


Fig. 22. Comparison of O KLL and N KLL Auger spectra from NO gas[258] and NO adsorbed on Ru(0001) at low temperatures and then warmed to 468 K. On warming the NO is seen to dissociate as shown by the similarity of O KLL spectra to those of chemisorbed oxygen shown in Fig. 23. The dissociated NO spectra are similar to those of NO on W(110) where dissociative adsorption is found at both 100 K and 300 K.[249] (From ref. 252).